Letter

Fractional quantum Hall edge polaritons

Lucas Winter* and Oded Zilberberg
Fachbereich Physik, Universität Konstanz, DE-78457 Konstanz, Germany

(Received 24 August 2023; revised 3 November 2025; accepted 10 November 2025; published 4 December 2025)

It is commonly believed that light cannot couple to the collective excitations of the fractional quantum Hall effect (FQHE). This assumption relies on Kohn's theorem that states that electron-electron interactions decouple from homogeneous electromagnetic fields due to Galilean invariance. Here, we demonstrate that light-matter coupling beyond the dipole approximation circumvents Kohn's theorem, and enables the coupling of cavity photons to the plasmonic edge modes of the FQHE. We derive the coupling using the FQHE bulk-boundary correspondence and predict the formation of experimentally detectable plasmon polaritons. In conjunction with recent experiments, we find that a single cavity mode leaves the system's topological protection intact. Interestingly, however, a multimode cavity mediates plasmon backscattering and effectively transforms the edges of the two-dimensional (2D) FQHE into a 1D wire. Such cavity-meditated nonlocal backscattering bodes the breakdown of the topological protection in the regime of ultrastrong photon-plasmon coupling. Our analytical framework and findings pave the way for investigating the topological order of the FQHE via optical spectroscopic probes as well as provide opportunities to control FQHE edge excitations using light.

DOI: 10.1103/qc6z-87c6

One of the most fascinating effects in condensed matter physics is the emergence of collective excitations arising from strong interactions between particles [1,2]. A principal setting for the formation of such exotic quasiparticles is the fractional quantum Hall effect (FQHE) [3–8]. Here, electrons with charge e and mass m are confined to move in two dimensions (2D) in the presence of a perpendicular magnetic field B. The competition between their kinetic energy and the magnetic field suppresses the dispersion, and leads to cyclotron motion at frequency $\omega_c = eB/m$. As a result, a highly degenerate Landau-level spectrum with gaps $\hbar\omega_c$ manifests. In this setting, electron-electron interactions can dominate and open a many-body gap at specific fractional fillings of the Landau levels, where new quasiparticles emerge. These collective excitations are dubbed anyons and are predicted to obey fractional exchange statistics, i.e., they are neither bosonics nor fermionic [7,9,10], and can even be used for topological quantum computation [11,12]. At so-called Laughlin fillings $\nu = 1/(2p+1)$ with $p \in \mathbb{N}$ [3,13,14], the resulting FQHE is well described using composite fermions (CFs) that support anyonic bulk excitations with energy scales on the order of the Coulomb energy $\sim e^2/(\epsilon l_B)$, where ϵ is the dielectric constant and l_B is the magnetic length [6].

Strong light-matter coupling in optical cavities can also lead to interesting collective excitations and effects [15–17]. For example, it allows for novel topological phases populated by light-matter hybrid particles known as polaritons [18,19]. In relation to the quantum Hall effect, coupling to light was used both for probing and for modifying the topological order using cavities [20–27]. In the noninteracting limit, and using very high frequencies, transitions between Landau levels were studied, leading to the formation of Landau polaritons [28–31], and modification of the quantized electron transport of the integer quantum Hall effect (IQHE) [32–34]. In essence, cavity vacuum fluctuations tend to expunge the quantized Hall transport in the IQHE [34–38]. Moving to the FQHE, its topological order can be probed indirectly by Landau polaritons [39,40]. Furthermore, the induction of bulk anyonic excitations by locally inserting angular momentum with electric fields has been proposed [41]. However, in experiments, the FQHE shows significant resilience to such coupling [35]. This resilience stems from Kohn's theorem, which states that a homogeneous electromagnetic field only modifies the center of motion dynamics while leaving electron-electron correlations intact [6,35,38,42,43]. For the same reason, the topological order seems to be protected from cavity vacuum fluctuation [35,38].

In realistic scenarios, Hall systems are finite. Due to the so-called bulk-boundary correspondence, in the noninteracting limit, chiral electronic edge modes appear in the gaps between the Landau levels, which carry the IQHE current [44,45]. Crucial to this work, a similar bulk-boundary correspondence manifests for the CFs, and carries the fractionally quantized current of the FQHE [7]. At the edge, we then expect chiral collective bosonic excitations (plasmonic modes), which fill the gaps between the effective CF Landau levels [46,47].

In this Letter, we derive a model for the coupling between cavity light and the FQHE. Our theory breaks Kohn's theorem by considering spatially varying mode profiles beyond the dipole approximation. Our derivation harnesses the

*Contact author: lucas.s.winter@icloud.com

Published by the American Physical Society under the terms of the Creative Commons Attribution 4.0 International license. Further distribution of this work must maintain attribution to the author(s) and the published article's title, journal citation, and DOI.

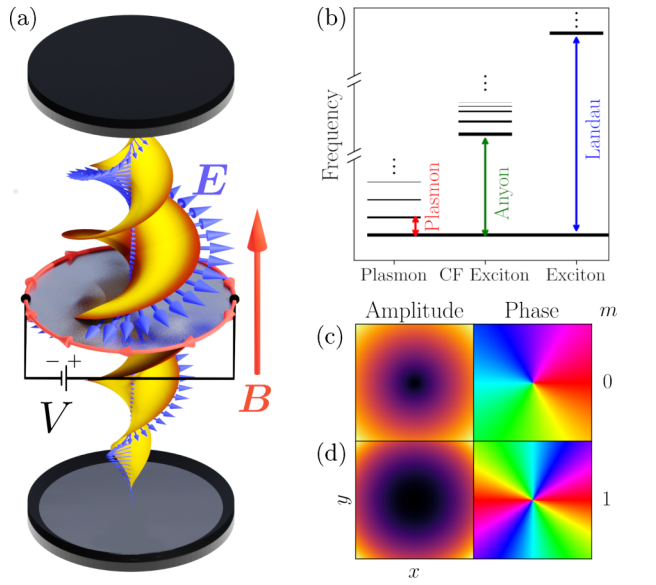


FIG. 1. System. (a) A 2D Hall disk is positioned inside an optical cavity [cf. Eq. (1)]. The Hall disk is subjected to a perpendicular magnetic field $\boldsymbol{B}$ and is coupled to a cavity electric field $\boldsymbol{E}$, which can be decomposed into angular momentum modes l [cf. Eq. (2)]. We show a single circularly polarized basis mode $\boldsymbol{E}_l$ (blue arrows) with a helical wave front (orange surface). A voltage bias V can be applied across the edge of the Hall bar. Here, we consider mesoscopic systems with $\nu = 1/3$ and $n = 10^{11}$ cm^{-2}: $B \approx 12.4$ T, $\ell_B \approx 7$ nm; circumference $L = 100$ μm. (b) The hierarchy of energy scales of the Hall effect, corresponding to potential excitation by the cavity, ranges from small to large energies: FQHE edge plasmons (red), FQHE bulk excitations (green), and IQHE Landau-level spacing (blue). (c) and (d) Examples of the cavity basis mode's amplitude and phase in the plane of the Hall disk for different orbital angular momentum (OAM) quanta m [cf. Eq. (2)].

bulk-boundary correspondence and implies strong coupling with the system's plasmonic edge modes. As a result, experimentally observable edge polaritons appear. Correspondingly, the cavity introduces backscattering between the edge modes on the opposite sides of the system, which can impact the Hall conductance. In agreement with experiments [35], within our model, a homogeneous cavity mode is insufficient to disturb the quantized Hall conductance. Crucially, however, we find that an inhomogeneous multimode cavity introduces numerous scattering channels and removes the topological protection. Our predictions offer a variety of observations that are within experimental reach. At the same time, our methodology can be applied to a plethora of other topological systems in mesoscopics, as well as to quantum simulators.

We consider an optical cavity coupled to a spin-polarized 2D electron gas (2DEG) in the FQHE regime [see Fig. 1(a)],

$$H_C = \frac{1}{2m_e}\sum_j [\boldsymbol{\pi}_j - e\boldsymbol{A}(\boldsymbol{r}_j)]^2 + V_{\text{int}} + V_{\text{conf}} + H_{\text{cav}}, \quad (1)$$

where $\boldsymbol{\pi}_j = \boldsymbol{p}_j - eBx_j\hat{\boldsymbol{e}}_y$ is the canonical momentum of electron j moving in the plane with momentum $\boldsymbol{p}_j$ in the presence of a perpendicular magnetic field B. The latter is written in Landau's gauge. The light-matter coupling involves the cavity vector potential $\boldsymbol{A}(\boldsymbol{r})$ using standard minimal coupling [6]. We allow $\boldsymbol{A}(\boldsymbol{r})$ to vary arbitrarily in space, to accommodate any electromagnetic environment. The terms V_{int} and V_{conf} are the electrons' Coulomb interaction and confinement potentials, respectively. The term $H_{\text{cav}} = \sum_{l\neq 0}\hbar\omega_{c,l}a_l^\dagger a_l$ describes a multimode cavity with mode frequencies $\omega_{c,l}$ and quantized annihilation operators a_l. In Fig. 1(b), we summarize the hierarchy of energy scales of the FQHE [cf. Eq. (1) in the absence of the cavity], and the discussion in the introduction.

For simplicity, we assume the Hall system to be rotationally symmetric around the cavity axis. This implies that the total electron angular momentum is conserved. As the angular momentum l is a good quantum number for the electrons, we write the electromagnetic field also in terms of angular momentum modes l. Radially, we use a basis of Hypergeometric-Gaussian modes [48,49], and assume, in the main text, a broad beam waist relative to the Hall system extent [50]

$$\boldsymbol{A} = \sum_{l\neq 0}\boldsymbol{A}_l = \sum_{l\neq 0} A_l[\boldsymbol{\epsilon} z^{|l|-1}\alpha_l + \boldsymbol{\epsilon}^*(z^*)^{|l|-1}\alpha_l^\dagger], \quad (2)$$

where $\boldsymbol{\epsilon} = (1, i, 0)^T/\sqrt{2}$ is the circular polarization vector and $z = (x + iy)/R$ encodes the position in the 2DEG using a complex coordinate, where R denotes the radius of the disk. The bosonic operators $\alpha_l = a_l\Theta(l) + a_l^\dagger\Theta(-l)$ and $\alpha_l^\dagger = a_l^\dagger\Theta(l) + a_l\Theta(-l)$ create or annihilate a photon with angular momentum l. The total photon angular momentum consists of one *quantum spin angular momentum* (SAM) and $m = l - 1$ quanta of *orbital angular momentum* (OAM) [51,52] [see Figs. 1(c) and 1(d)]. Modes with $|l| > 1$ are inhomogeneous and break Kohn's theorem. Note that the coupling of any 3D cavity field to a 2DEG can be written in the form of Eq. (2) by applying a suitable gauge transform [50].

In the following, we develop a, relevant for DC transport, low-energy effective theory focused on coupling to the plasmonic edge excitations. We truncate matrix elements that couple to high energies [cf. Fig. 1(b)], i.e., our theory is valid for energies below the many-body gap. Our model (1), however, is written in the Coulomb gauge, which is less robust to level truncation than the dipole gauge [53,54]. Hence, we switch to the dipole gauge using the unitary transformation $H_D = UH_CU^\dagger$ with $U = \prod_j \exp[-ie\sum_{l\neq 0}\boldsymbol{A}_l(\boldsymbol{r}_j)\cdot\boldsymbol{r}_j/(|l|\hbar)]$ [53,55],

$$H_D = \sum_j\left[\frac{\boldsymbol{\pi}_j^2}{2m_e} + \sum_{l\neq 0}\frac{e}{|l|}\boldsymbol{E}_l(\boldsymbol{r}_j)\cdot\boldsymbol{r}_j\right] + V_{\text{int}} + V_{\text{conf}} + H_{\text{cav}}. \quad (3)$$

Here, $\boldsymbol{E}_l\cdot\boldsymbol{r} = iA_l\omega_{c,l}(p_l\alpha_l - p_l^*\alpha_l^\dagger)$ is the dipole coupling of the l component of the electric field, and $p_l = \sum_j z_j^l$ is a symmetric polynomial in the electron coordinates $\{z_j\}$. We omit the dipole self-energy, which only renormalizes the parameters of our theory and vanishes in the thermodynamic limit [50].

When the FQHE system absorbs a photon $a_l^\dagger$ [see Fig. 2(a)], angular momentum conservation dictates a transition to an excited state, with more angular momentum than the Laughlin ground state. We express the Hamiltonian (3) in the basis of many-body angular momentum states. In-

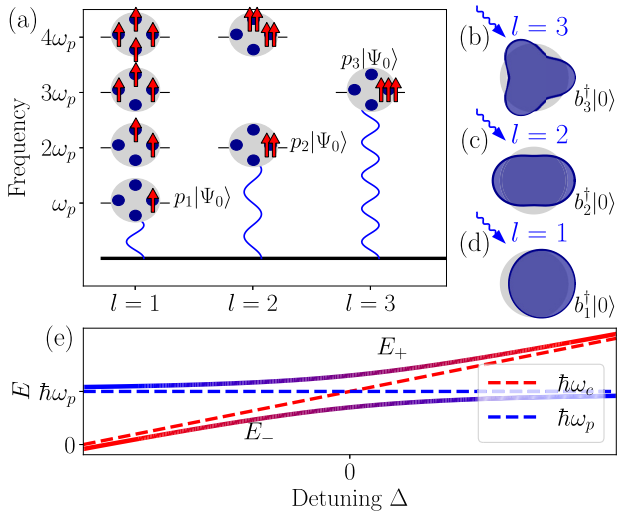


FIG. 2. Light-matter coupling to the FQHE and formation of edge plasmon polaritons. (a) Low-energy spectrum of the FQH disk (with four electrons for illustration). Excited states are obtained by attaching one or more angular momentum quanta (red arrows) to electrons (blue circles). A single angular momentum quanta increases the energy by $\hbar\omega_p$ units. Absorbed photons attach or remove angular momentum quanta from single electrons, via optical transitions (squiggly lines) into states $p_l|\Psi_0\rangle$, where $l=1,2,3$ are marked. (b)–(d) According to the bulk-boundary correspondence, bulk states with added angular momentum $p_l|\Psi_0\rangle$ manifest as edge plasmons $b_l^\dagger|0\rangle$. Photons with angular momentum l (squiggly line) can create plasmons at wave vector $k_l = 2\pi l/L$. (e) FQHE edge excitations spectrum in a single-mode cavity field shows plasmon-polariton anticrossing with cavity detuning [cf. Eq. (5)]. Dashed lines indicate the spectrum without a light-matter interaction.

creasing the angular momentum of one electron by l units corresponds to multiplying the ground state with the symmetric polynomial $p_l|\Psi_0\rangle$ [13,56–59], where $p_l = \sum_j z_j^l$. A general excited state can then be written as $|\Psi_{\boldsymbol{\lambda}}\rangle = \prod_l p_n^{\lambda_l}|\Psi_0\rangle$. Each quantum of angular momentum adds energy $\hbar\omega_p$, where ω_p is the plasmon frequency [see Fig. 2(a)]. The matrix elements of the light-matter coupling in the many-body basis $|\Psi_{\boldsymbol{\lambda}}\rangle$ therefore read

$$\begin{aligned}\langle\Psi_{\boldsymbol{\lambda}}|H_{\rm int}|\Psi_{\boldsymbol{\mu}}\rangle &= \int\prod dz_j \Psi^*_{\boldsymbol{\lambda}}(\{z_j\})H_{\rm int}\Psi_{\boldsymbol{\mu}}(\{z_j\}) \\ &= i\sum_{l\neq 0}\frac{eE_l}{|l|}(\langle\Psi_{\boldsymbol{\lambda}}|p_{|l|}|\Psi_{\boldsymbol{\mu}}\rangle\alpha_l - \langle\Psi_{\boldsymbol{\lambda}}|p_{|l|}|\Psi_{\boldsymbol{\mu}}\rangle^*\alpha_l^\dagger), \quad (4)\end{aligned}$$

with $E_l = A_l\omega_{c,l}$. Note that the inner products are evaluated by taking real-space integrals over the many-body Laughlin wave function [50]. In our case, we can use the fact that $\langle\Psi_{\boldsymbol{\lambda}}\rangle$ form an orthogonal basis $\langle\Psi_{\boldsymbol{\lambda}}|p_l|\Psi_{\boldsymbol{\mu}}\rangle \propto +\delta(\lambda_l-\mu_l+1)\prod_{n\neq l}\delta(\lambda_n-\mu_n)$ to simplify the calculation [57]. This implies that an absorbed photon $a_l^\dagger$ attaches l quanta of angular momentum to one electron, and induces a transition into an excited state [see Fig. 2(a)].

In the thermodynamic limit, the bulk-edge correspondence specifically states that the inner product between bulk wave functions is directly related with the inner product between edge states $\langle\Psi_{\boldsymbol{\lambda}}|\Psi_{\boldsymbol{\mu}}\rangle = \sqrt{\nu l}\,L/(2\pi)\langle\boldsymbol{\mu}|\boldsymbol{\lambda}\rangle$ [46,57], where ν is the filling factor $\nu = n_{\rm 2D}h/(eB)$ corresponding to electron density $n_{\rm 2D}$, and L is the edge circumference. Note that in small systems corrections to the inner product relation will appear. Crucial to this work, the bulk-edge correspondence implies that the excited state $p_l|\Psi_0\rangle$ maps to a plasmonic surface wave at the edge $b_l^\dagger|0\rangle$, where $b_l^\dagger$ is a bosonic creation operator acting on an edge state; see Figs. 2(b)–2(d). Each plasmonic excitation is defined by its momentum $\hbar k_l = \hbar\frac{2\pi}{L}l$ and distinct energy $\hbar\omega_p l = \hbar v k_l$, with edge drift velocity v. The collective of all plasmonic excitations forms a chiral Luttinger liquid [46]. By using the bulk-edge relations, we evaluate the matrix elements and obtain an effective cavity-plasmon Hamiltonian

$$\begin{aligned}H_L = &\sum_{l\neq 0}\hbar\big[(\omega_p l)b_l^\dagger b_l + ib_l^\dagger\big(\Omega_l a_l + \Omega_{-l}a_{-l}^\dagger\big) + \text{H.c.}\big] \\ &+ H_{\rm cav} + V_{\rm anh}, \quad (5)\end{aligned}$$

with the light-matter coupling strength $\Omega_l = e/hE_lL\sqrt{\nu/|l|} = 2\omega_c/(\sqrt{|l|}\omega_{\rm cyc})\Omega_{\rm Rabi} \propto \sqrt{N_e}$, where $\Omega_{\rm Rabi} = eA_l\sqrt{N_e\hbar\omega_{\rm cyc}/(2m_e\hbar^2)}$ is the collective Rabi frequency [34]. This implies that an absorbed photon, with angular momentum l, creates an edge plasmon with linear momentum $k_l = 2\pi l/L$ [see Figs. 2(b)–2(d). Crucially, the total angular momentum is thus conserved, as the Hall system can absorb both SAM and OAM. $V_{\rm anh}$ incorporates anharmonic corrections to the confinement potential, coupling the $l=1$ center-of-motion plasmon mode with higher multipoles ($l>1$), thereby violating Kohn's theorem. However, these corrections scale at least as $O(1/N)$, making them negligible in the large-N limit [47,60]. The following points are important to note: (i) In the case of a cavity field with opposite chirality $l<0$ to that of the edge mode, we obtain a counterrotating coupling term $i\Omega_{-l}(b_l a_{-l} - b_l^\dagger a_{-l}^\dagger)$ in Eq. (5), indicating that an absorbed photon destroys a plasmon. (ii) In small systems, noncircular terms that mix different angular momenta appear in the Hamiltonian; these can be treated perturbativly within our theory [61]. (iii) Geometry: in the main text we focus on a disk, however, a similar diagonal Hamiltonians also apply to other geometries (Hall bar, Corbino), with geometry only entering via form factors (see Supplemental Material [50]). (iv) Including dipole self-energy slightly renormalizes the plasmon frequency and light-matter coupling [50]. Finally, (v) we can derive the same photon-plasmon coupling through a cavity-induced anomalous current [62].

Strong light-matter coupling typically leads to the formation of polaritons [16]. For simplicity, we first consider a single-mode cavity with an angular momentum l. This limit can be realized using chiral cavities, which are a topic of active experimental research [63]. Due to conservation of angular momentum, the cavity will couple solely to a single plasmon mode. We can diagonalize the Hamiltonian (5) via a Bogoliubov transform and obtain the polariton eigenenergies $2E_\pm = \hbar\omega_p l + \hbar\omega_c \pm \sqrt{\Delta^2 + 4\hbar^2\Omega_l^2}$, where $\Delta = \hbar(\omega_c - \omega_p l)$. The resulting spectrum reveals typical anticrossing [see Fig. 2(d)]. Importantly, the anticrossing can

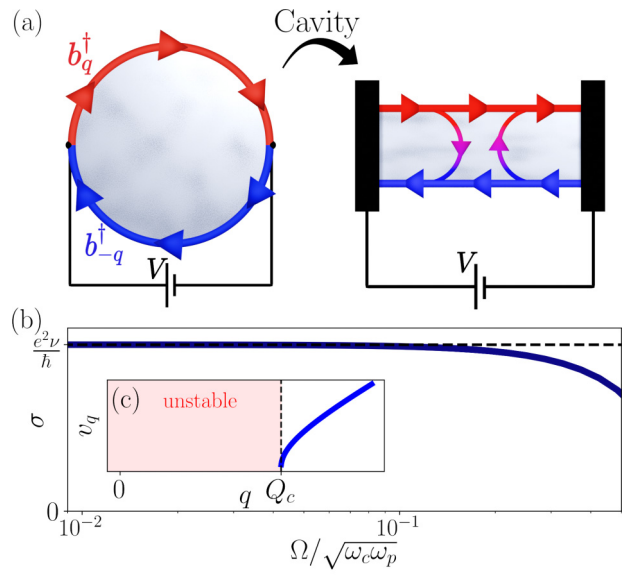


FIG. 3. Cavity-mediated breakdown of topological protection. (a) The plasmons around the disk can be decomposed into right-moving (red) and left-moving (blue) modes [cf. Eq. (6)]. Cavity-mediated interactions couple the right and left movers and transform the system into an effective 1D wire [cf. Eq. (7)]. (b) The Hall conductivity as a function of the normalized coupling strength [cf. Eq. (9)]. (c) Backscattering red-detunes the plasmon dispersion, which can make the plasmon polaritons unstable below the wave vector $Q_c = \frac{4\Omega^2}{\omega_c v}$.

be measured using spectroscopy experiments: using common experimental values [64–66], the edge drift velocity at $\nu = 1/3$ lies in $v \approx (2\text{–}4) \times 10^4$ m/s. For an edge circumference $L = 100$ μm, the fundamental edge plasmon has $k = 2\pi/L$ and wavelength $\lambda_p \simeq L$, giving $f_p = v/L \approx 0.2\text{–}0.4$ GHz ($\omega_p = 2\pi f_p$), well below the cyclotron frequency and the free-space light wavelength is $\lambda_{\text{light}} \approx 0.3$ m. Note that in the presence of polariton excitations, the Laughlin state $|\Psi_0\rangle$ is no longer the ground state, potentially leading to modified transport properties.

We next assess how coupling to the cavity mode affects conductivity, as measured at opposing points on the Hall disk. As Kohn's theorem is broken, the Hall plateaus may (but do not have to) be disrupted. The Ohmic contacts effectively partition the edge into two branches, one with left-moving ($q < 0$) and one with right-moving plasmonic excitations ($q > 0$) [see Fig. 3(a)]. Inverting the y axis ($\mathcal{T} : y \to -y$) morphs the left-moving edge into the right-moving edge. Correspondingly, applying $\mathcal{T}$ to the light-matter coupling Hamiltonian (5), yields the coupling to the left-moving edge. Additionally, applying the inversion to the plasmon wavefunction coordinates leads to complex conjugation $\mathcal{T}z = z^*$, so $\mathcal{T}b_q = b_{-q}^\dagger$. Together, the Hamiltonian containing both edges reads

$$H_{2E} = \sum_{q\neq 0} \hbar[v|q|\, b_q^\dagger b_q + i b_q^\dagger(\Omega_q a_{l_q} + \Omega_{-q} a_{-l_q}^\dagger) + \text{H.c.}] + H_{\text{cav}}. \tag{6}$$

Note, we neglect anharmonic corrections to the confinement potential. However, as these corrections do not affect universal properties such as conductivity and diminish with system size [47,60], we expect our results to hold across the entire Hall universality class. To ascertain the effective cavity-mediated coupling between the left- and right-moving edge states, we transform Eq. (6) using a Schrieffer-Wolff transformation

$$H_{\text{eff}} = \sum_{q\neq 0} \hbar|q| \left[[v + V(q)] b_q^\dagger b_q - \frac{1}{2} V(q)(b_q^\dagger b_{-q}^\dagger + b_q b_{-q}) \right]. \tag{7}$$

Here, $V(q) = -2\Omega^2\omega_c/[|q|(\omega_c^2 - v^2q^2)]$ with $\Omega = \Omega_1$ [50]. Importantly, we obtain the familiar Luttinger Hamiltonian for a 1D wire when the cavity is included already within second-order perturbation theory [67]. Specifically, the cavity introduces plasmon backscattering proportional to V [see Fig. 3(a)]. This is a key result of our work.

Using our effective (matter-only) model, we can compute the conductivity through the opposite edges of the device [see Fig. 1(a)]. To this end, we diagonalize the effective model (7) using a Bogoliubov transformation $b_q^\dagger = \cosh(\varphi_q)\beta_q^\dagger - \sinh(\varphi_q)\beta_{-q}$, where $\tanh(2\varphi_q) = V/(v + V)$, and b_q transforms accordingly [67]. In diagonal form, the model reads $H_{\text{eff}} = \sum_{q\neq 0} \hbar v_q |q| \beta_q^\dagger \beta_q$, with the plasmon dispersion $v_q = \sqrt{v^2 + 2vV}$. The current operator is defined by $j_q = (i/q)\partial_t n_q$, with n_q the electron density. In our case, the current operator linearized around small wave vectors reads $j_q = \sqrt{L|q|\nu/(2\pi)}v\,\text{sgn}(q)(\beta_q - \beta_{-q}^\dagger)$ [68]. Using Kubo's formula for small wave vectors, the conductivity then reads [69]

$$\sigma = \frac{e^2}{\hbar L} \lim_{\omega\to 0} \int_{-\infty}^{0} dx' \sum_{q\neq 0} e^{iq(x-x')} G_j(q,\omega), \tag{8}$$

where $G_j(q,\omega) = i\int_0^\infty dt\, \langle [j_q(t), n_{-q}(0)] \rangle e^{i(\omega+i\eta)t}$ is the retarded current-density correlation function, where we used the relation $\beta_q^\dagger(t) = e^{iv_q|q|t}\beta(0)$ [67].

We first consider a single-mode cavity with angular momentum $\pm l$, similar to that employed in a recent experiment [35,50],

$$\sigma = \frac{e^2\nu}{h} + \frac{e^2}{\hbar L} \sum_{q=\pm 2\pi/Ll} \frac{i}{q} e^{iq(x-x')} \lim_{\omega\to 0} (\tilde{G}_j - G_j) = \frac{e^2\nu}{h},$$

where $\tilde{G}_j$ is the current-density correlation function in the presence of the cavity and G_j is the one without it. The correlation function for individual plasmons vanishes in the DC limit $\lim_{\omega\to 0} \tilde{G}_j(\pm q_0, \omega) = 0$ if transport is measured a the ends of the edge $x - x' = L$. Crucially, for a homogeneous cavity mode $l = 1$ our result is consistent with Kohn's theorem and complies with recent transport experiments [35], as the conductivity is not modified by a homogeneous cavity mode, despite coupling to the edge excitations. Note that we consider a fully coherent (Hamiltonian) system, where no current can be dissipated; a dissipative cavity or edge disorder may lead to a weaking of the topological protection [34,38].

Next, we consider a multimode cavity with highly inhomogeneous mode profiles, disrupting Kohn's theorem.

Specifically, we consider a "pizza-slice aperture" by reducing the azimuthal angle $\Delta\phi$ [70]. This increases the uncertainty in the angular momentum ΔL, e.g., as $\Delta L \cdot \Delta\phi \geqslant \hbar/2$ due to the uncertainty relation, and thus all photon modes participate equally $A_l \to 1$ in Eq. (2). Given the continuum of modes, we can replace the sum over q in Eq. (8) with an integral, and obtain using the residue theorem [50]

$$\sigma = \frac{e^2\nu}{h}\sqrt{1 - \frac{4\Omega^2}{\omega_c\omega_p}}. \tag{9}$$

In this inhomogeneous limit, as the light-matter coupling strength Ω increases, the conductivity deviates from the universal value $e^2\nu/h$, leading to the destruction of conductivity quantization [see Fig. 3(b)]. The cavity-induced backscattering lifts the chiral protection of the edge modes, thus allowing charges on the opposite edges of the 2D bulk to screen each other. Specifically, the cavity modifies the plasmon dispersion to $v_q = v\sqrt{1 - 4\Omega^2/(|q|\omega_c v)}$. Furthermore, plasmons with a wave vector below $|q| \leqslant Q_c = 4\Omega^2/(\omega_c v)$ redshift and can become unstable [see Fig. 3(c)], signaling a potential phase transition in the system. What phase appears beyond the instability is beyond the scope of our model. Please note this result specifically applies to multimode cavities and is therefore fully consistent with recent experiments indicating that Hall plateaus are enhanced for a single homogeneous cavity mode [71].

Three key implications of our result involve (i) the cavity modes can form polaritons with the plasmonic edges of the FQHE, (ii) a homogeneous mode is insufficient for impacting the topological protection, and (iii) an inhomogeneous multimode cavity can destroy the Hall plateaus. The latter is a result of light-induced backscattering between opposite edges of the Hall system. Our model provides a versatile platform for studying light-matter interaction in the FQHE, which can be readily extended to other filling fractions $\nu = 1/(2p+1)$, with multiple edge modes [47]. We anticipate similar coupling between light and topological boundary modes in other systems that exhibit the chiral anomaly. Taking into account realistic experimental values, our predictions are within reach of experimental observation, and motivate spectroscopic methods for probing the topological order of the FQHE, as well as assist in resolving long-standing controversies concerning the system's edge structure [72,73]. Interestingly, the decay of the edge plasmons into photons opens up the potential of controlling the orbital angular momentum of light. Beyond mesoscopics, our model can be applied cold atomic systems, as well as other quantum simulators [74–77].

We thank S. Simon, P. Rabl, C. Ciuti, and I. Carusotto for fruitful discussions. The authors acknowledge financial support from the Deutsche Forschungsgemeinschaft (DFG) - Projects No. 449653034 and No. SFB1432.

[1] I. V. Lerner, B. L. Althsuler, V. I. Falko, and T. Giamarchi, *Strongly Correlated Fermions and Bosons in Low-Dimensional Disordered Systems* (Springer Science & Business Media, Dordrecht, 2002), Vol. 72.

[2] E. Dagotto, Complexity in strongly correlated electronic systems, Science **309**, 257 (2005).

[3] D. C. Tsui, H. L. Stormer, and A. C. Gossard, Two-Dimensional magnetotransport in the extreme quantum limit, Phys. Rev. Lett. **48**, 1559 (1982).

[4] J. Fröhlich and U. M. Studer, Gauge invariance and current algebra in nonrelativistic many-body theory, Rev. Mod. Phys. **65**, 733 (1993).

[5] H. L. Stormer, D. C. Tsui, and A. C. Gossard, The fractional quantum Hall effect, Rev. Mod. Phys. **71**, S298 (1999).

[6] J. K. Jain, *Composite Fermions* (Cambridge University Press, Cambridge, UK, 2007).

[7] A. Stern, Anyons and the quantum Hall effect—a pedagogical review, Ann. Phys. **323**, 204 (2008).

[8] J. Fröhlich, Gauge invariance and anomalies in condensed matter physics, J. Math. Phys. **64**, 031903 (2023).

[9] G. Campagnano, O. Zilberberg, I. V. Gornyi, D. E. Feldman, A. C. Potter, and Y. Gefen, Hanbury brown–twiss interference of anyons, Phys. Rev. Lett. **109**, 106802 (2012).

[10] G. Campagnano, O. Zilberberg, I. V. Gornyi, and Y. Gefen, Hanbury brown and twiss correlations in quantum Hall systems, Phys. Rev. B **88**, 235415 (2013).

[11] C. Nayak, S. H. Simon, A. Stern, M. Freedman, and S. Das Sarma, Non-Abelian anyons and topological quantum computation, Rev. Mod. Phys. **80**, 1083 (2008).

[12] O. Zilberberg, B. Braunecker, and D. Loss, Controlled-NOT gate for multiparticle qubits and topological quantum computation based on parity measurements, Phys. Rev. A **77**, 012327 (2008).

[13] R. B. Laughlin, Anomalous quantum Hall effect: An incompressible quantum fluid with fractionally charged excitations, Phys. Rev. Lett. **50**, 1395 (1983).

[14] H. L. Stormer, Nobel lecture: The fractional quantum Hall effect, Rev. Mod. Phys. **71**, 875 (1999).

[15] M. Fleischhauer, A. Imamoglu, and J. P. Marangos, Electromagnetically induced transparency: Optics in coherent media, Rev. Mod. Phys. **77**, 633 (2005).

[16] I. Carusotto and C. Ciuti, Quantum fluids of light, Rev. Mod. Phys. **85**, 299 (2013).

[17] J. Bloch, I. Carusotto, and M. Wouters, Non-equilibrium Bose–Einstein condensation in photonic systems, Nat. Rev. Phys. **4**, 470 (2022).

[18] T. Ozawa, H. M. Price, A. Amo, N. Goldman, M. Hafezi, L. Lu, M. C. Rechtsman, D. Schuster, J. Simon, O. Zilberberg, and I. Carusotto, Topological photonics, Rev. Mod. Phys. **91**, 015006 (2019).

[19] D. D. Solnyshkov, G. Malpuech, P. St-Jean, S. Ravets, J. Bloch, and A. Amo, Microcavity polaritons for topological photonics, Opt. Mater. Express **11**, 1119 (2021).

[20] F. Schlawin, D. M. Kennes, and M. A. Sentef, Cavity quantum materials, Appl. Phys. Rev. **9**, 011312 (2022).
[21] A. Frisk Kockum, A. Miranowicz, S. De Liberato, S. Savasta, and F. Nori, Ultrastrong coupling between light and matter, Nat. Rev. Phys. **1**, 19 (2019).
[22] P. Forn-Díaz, L. Lamata, E. Rico, J. Kono, and E. Solano, Ultrastrong coupling regimes of light-matter interaction, Rev. Mod. Phys. **91**, 025005 (2019).
[23] T. Jaako, Z.-L. Xiang, J. J. Garcia-Ripoll, and P. Rabl, Ultrastrong-coupling phenomena beyond the Dicke model, Phys. Rev. A **94**, 033850 (2016).
[24] M. Ruggenthaler, N. Tancogne-Dejean, J. Flick, H. Appel, and A. Rubio, From a quantum-electrodynamical light–matter description to novel spectroscopies, Nat. Rev. Chem. **2**, 0118 (2018).
[25] F. J. Garcia-Vidal, C. Ciuti, and T. W. Ebbesen, Manipulating matter by strong coupling to vacuum fields, Science **373**, eabd0336 (2021).
[26] M. A. Sentef, M. Ruggenthaler, and A. Rubio, Cavity quantum-electrodynamical polaritonically enhanced electron-phonon coupling and its influence on superconductivity, Sci. Adv. **4**, eaau6969 (2018).
[27] P. Kirton, M. M. Roses, J. Keeling, and E. G. Dalla Torre, Introduction to the Dicke model: From equilibrium to nonequilibrium, and vice versa, Adv. Quantum Technol. **2**, 1800043 (2019).
[28] D. Hagenmüller, S. De Liberato, and C. Ciuti, Ultrastrong coupling between a cavity resonator and the cyclotron transition of a two-dimensional electron gas in the case of an integer filling factor, Phys. Rev. B **81**, 235303 (2010).
[29] G. Scalari, C. Maissen, D. Turčinková, D. Hagenmüller, S. De Liberato, C. Ciuti, C. Reichl, D. Schuh, W. Wegscheider, M. Beck, and J. Faist, Ultrastrong coupling of the cyclotron transition of a 2D electron gas to a THz metamaterial, Science **335**, 1323 (2012).
[30] J. Keller, G. Scalari, F. Appugliese, S. Rajabali, M. Beck, J. Haase, C. A. Lehner, W. Wegscheider, M. Failla, M. Myronov, D. R. Leadley, J. Lloyd-Hughes, P. Nataf, and J. Faist, Landau polaritons in highly nonparabolic two-dimensional gases in the ultrastrong coupling regime, Phys. Rev. B **101**, 075301 (2020).
[31] X. Li, M. Bamba, Q. Zhang, S. Fallahi, G. C. Gardner, W. Gao, M. Lou, K. Yoshioka, M. J. Manfra, and J. Kono, Vacuum bloch–Siegert shift in Landau polaritons with ultra-high cooperativity, Nat. Photonics **12**, 324 (2018).
[32] N. Bartolo and C. Ciuti, Vacuum-dressed cavity magnetotransport of a two-dimensional electron gas, Phys. Rev. B **98**, 205301 (2018).
[33] G. L. Paravicini-Bagliani, F. Appugliese, E. Richter, F. Valmorra, J. Keller, M. Beck, N. Bartolo, C. Rössler, T. Ihn, K. Ensslin, C. Ciuti, G. Scalari, and J. Faist, Magneto-transport controlled by Landau polariton states, Nat. Phys. **15**, 186 (2019).
[34] C. Ciuti, Cavity-mediated electron hopping in disordered quantum Hall systems, Phys. Rev. B **104**, 155307 (2021).
[35] F. Appugliese, J. Enkner, G. L. Paravicini-Bagliani, M. Beck, C. Reichl, W. Wegscheider, G. Scalari, C. Ciuti, and J. Faist, Breakdown of topological protection by cavity vacuum fields in the integer quantum Hall effect, Science **375**, 1030 (2022).
[36] V. Rokaj, M. Penz, M. A. Sentef, M. Ruggenthaler, and A. Rubio, Quantum electrodynamical Bloch theory with homogeneous magnetic fields, Phys. Rev. Lett. **123**, 047202 (2019).
[37] V. Rokaj, M. Penz, M. A. Sentef, M. Ruggenthaler, and A. Rubio, Polaritonic hofstadter butterfly and cavity control of the quantized Hall conductance, Phys. Rev. B **105**, 205424 (2022).
[38] V. Rokaj, J. Wang, J. Sous, M. Penz, M. Ruggenthaler, and A. Rubio, Weakened topological protection of the quantum Hall effect in a cavity, Phys. Rev. Lett. **131**, 196602 (2023).
[39] P. Knüppel, S. Ravets, M. Kroner, S. Fält, W. Wegscheider, and A. Imamoglu, Nonlinear optics in the fractional quantum Hall regime, Nature (London) **572**, 91 (2019).
[40] P. Knüppel, Two-dimensional polaron-polaritons: Interactions and transport, Ph.D. thesis, ETH Zurich, 2021.
[41] T. Graß, M. Gullans, P. Bienias, G. Zhu, A. Ghazaryan, P. Ghaemi, and M. Hafezi, Optical control over bulk excitations in fractional quantum Hall systems, Phys. Rev. B **98**, 155124 (2018).
[42] W. Kohn, Cyclotron resonance and de Haas–van Alphen oscillations of an interacting electron gas, Phys. Rev. **123**, 1242 (1961).
[43] T. Maag, A. Bayer, S. Baierl, M. Hohenleutner, T. Korn, C. Schüller, D. Schuh, D. Bougeard, C. Lange, R. Huber, M. Mootz, J. E. Sipe, S. W. Koch, and M. Kira, Coherent cyclotron motion beyond Kohn's theorem, Nat. Phys. **12**, 119 (2016).
[44] R. B. Laughlin, Quantized Hall conductivity in two dimensions, Phys. Rev. B **23**, 5632 (1981).
[45] B. I. Halperin, Quantized Hall conductance, current-carrying edge states, and the existence of extended states in a two-dimensional disordered potential, Phys. Rev. B **25**, 2185 (1982).
[46] X. G. Wen, Chiral luttinger liquid and the edge excitations in the fractional quantum Hall states, Phys. Rev. B **41**, 12838 (1990).
[47] X.-G. Wen, Theory of the edge states in fractional quantum Hall effects, Int. J. Mod. Phys. B **06**, 1711 (1992).
[48] V. V. Kotlyar, R. V. Skidanov, S. N. Khonina, and V. A. Soifer, Hypergeometric modes, Opt. Lett. **32**, 742 (2007).
[49] E. Karimi, G. Zito, B. Piccirillo, L. Marrucci, and E. Santamato, Hypergeometric-Gaussian modes, Opt. Lett. **32**, 3053 (2007).
[50] See Supplemental Material at http://link.aps.org/supplemental/10.1103/qc6z-87c6 for more details, which includes Refs. [67,68].
[51] M. Padgett, J. Courtial, and L. Allen, Light's orbital angular momentum, Phys. Today **57**(5), 35 (2004).
[52] K. A. Forbes and D. L. Andrews, Orbital angular momentum of twisted light: Chirality and optical activity, J. Phys.: Photonics **3**, 022007 (2021).
[53] D. De Bernardis, P. Pilar, T. Jaako, S. De Liberato, and P. Rabl, Breakdown of gauge invariance in ultrastrong-coupling cavity QED, Phys. Rev. A **98**, 053819 (2018).
[54] O. Di Stefano, A. Settineri, V. Macrì, L. Garziano, R. Stassi, S. Savasta, and F. Nori, Resolution of gauge ambiguities in ultrastrong-coupling cavity quantum electrodynamics, Nat. Phys. **15**, 803 (2019).
[55] J. D. Jackson, From Lorenz to Coulomb and other explicit gauge transformations, Am. J. Phys. **70**, 917 (2002).
[56] F. Duncan and M. Haldane, The hierarchy of fractional states and numerical studies, in *The Quantum Hall Effect*, edited by R. E. Prange and S. M. Girvin, Graduate Texts in Contemporary Physics (Springer, New York, 1990), pp. 303–352.
[57] S. H. Simon, Wavefunctionology: The special structure of certain fractional quantum Hall wavefunctions, in *Fractional*

Quantum Hall Effects (World Scientific, Singapore, 2020), pp. 377–434.

[58] T. H. Hansson, C.-C. Chang, J. K. Jain, and S. Viefers, Conformal field theory of composite fermions, Phys. Rev. Lett. **98**, 076801 (2007).

[59] T. H. Hansson, M. Hermanns, S. H. Simon, and S. F. Viefers, Quantum Hall physics: Hierarchies and conformal field theory techniques, Rev. Mod. Phys. **89**, 025005 (2017).

[60] A. Nardin and I. Carusotto, Linear and nonlinear edge dynamics of trapped fractional quantum Hall droplets, Phys. Rev. A **107**, 033320 (2023).

[61] R. Fern, R. Bondesan, and S. H. Simon, Effective edge state dynamics in the fractional quantum Hall effect, Phys. Rev. B **98**, 155321 (2018),.

[62] L. Winter and O. Zilberberg (unpublished).

[63] H. Hübener, U. De Giovannini, C. Schäfer, J. Andberger, M. Ruggenthaler, J. Faist, and A. Rubio, Engineering quantum materials with chiral optical cavities, Nat. Mater. **20**, 438 (2021).

[64] F. E. Camino, W. Zhou, and V. J. Goldman, Transport in the laughlin quasiparticle interferometer: Evidence for topological protection in an anyonic qubit, Phys. Rev. B **74**, 115301 (2006).

[65] C. Lin, M. Hashisaka, T. Akiho, K. Muraki, and T. Fujisawa, Quantized charge fractionalization at quantum Hall Y junctions in the disorder dominated regime, Nat. Commun. **12**, 131 (2021).

[66] M. P. Röösli, M. Hug, G. Nicolí, P. Märki, C. Reichl, B. Rosenow, W. Wegscheider, T. Ihn, and K. Ensslin, Characterization of quasiparticle tunneling in a quantum dot from temperature dependent transport in the integer and fractional quantum Hall regime, arXiv:2112.11935.

[67] G. Giuliani and G. Vignale, *Quantum Theory of the Electron Liquid* (Cambridge University Press, Cambridge, UK, 2005).

[68] J. von Delft and H. Schoeller, Bosonization for beginners—refermionization for experts, Ann. Phys. **510**, 225 (1998).

[69] H. Bruus and K. Flensberg, *Many-Body Quantum Theory in Condensed Matter Physics*, Oxford Graduate Texts (Oxford University Press, Oxford, UK, 2004).

[70] S. Franke-Arnold, S. M. Barnett, E. Yao, J. Leach, J. Courtial, and M. Padgett, Uncertainty principle for angular position and angular momentum, New J. Phys. **6**, 103 (2004).

[71] J. Enkner, L. Graziotto, D. Boriçi, F. Appugliese, C. Reichl, G. Scalari, N. Regnault, W. Wegscheider, C. Ciuti, and J. Faist,, Tunable vacuum-field control of fractional and integer quantum Hall phases, Nature (London) **641**, 884 (2025).

[72] M. D. Johnson and A. H. MacDonald, Composite edges in the $\nu = 2/3$ fractional quantum Hall effect, Phys. Rev. Lett. **67**, 2060 (1991).

[73] X.-G. Wen, Topological orders and edge excitations in FQH states, Adv. Phys. **44**, 405 (1995).

[74] J. Léonard, S. Kim, J. Kwan, P. Segura, F. Grusdt, C. Repellin, N. Goldman, and M. Greiner, Realization of a fractional quantum Hall state with ultracold atoms, Nature (London) **619**, 495 (2023).

[75] P. Kumar, T. Biswas, K. Feliz, R. Kanamoto, M.-S. Chang, A. K. Jha, and M. Bhattacharya, Cavity optomechanical sensing and manipulation of an atomic persistent current, Phys. Rev. Lett. **127**, 113601 (2021).

[76] P. Di Francesco, P. Mathieu, and D. Sénéchal, *Conformal Field Theory*, Graduate Texts in Contemporary Physics (Springer, New York, 1997).

[77] D. Tong, Lectures on the quantum Hall effect, arXiv:1606.06687.